Surface effects on functional amyloid formation – Supplementary Information

Alexander J. Dear,[a,d] Georg Meisl,[a] Christopher G. Taylor,[a] Umberto Capasso Palmiero,[b] Susanne Nordby Stubbe,[c] Qian Liu,[c] Paolo Arosio,[b] Sara Linse,[d] Tuomas P. J. Knowles[a] and Maria Andreasen[c]

[a]Yusuf Hamied Department of Chemistry, University of Cambridge, Lensfield Road, Cambridge CB2 1EW, UK
[b]Institute for Chemical and Bioengineering, Department of Chemistry and Applied Biosciences, ETH Zürich, Zürich, Switzerland
[c]Department of Biomedicine, Aarhus University, Wilhelm Meyers Allé 3, Aarhus DK-8000, Denmark
[d]Department of Biochemistry and Structural Biology, Lund University, SE-221 00, Lund, Sweden

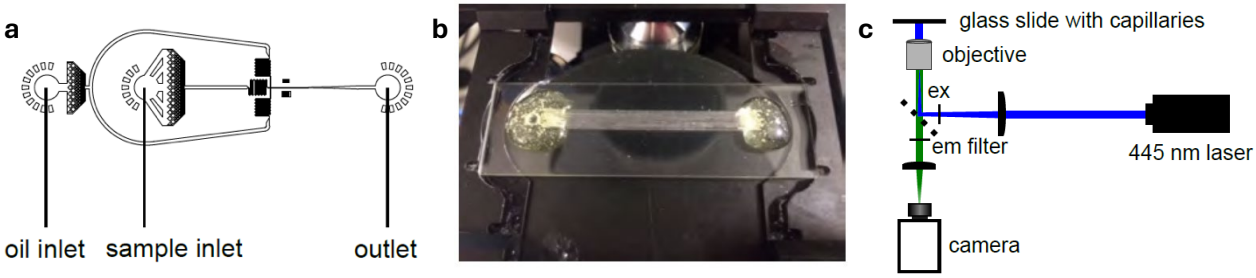

Supplementary Figure 1. Experimental setup of aggregation in microdroplet. A: Design of the microfluidic flow focusing device for droplet generation. Oil and sample inlets as well as outlet for droplet collection are highlighted. **B**: The capillaries containing droplets with different FapC monomeric concentration were sealed with wax and glued on a glass slide for imaging. **C**: Schematic illustration of the laser setup used for monitoring the fluorescence intensity of the microdroplets. The glass slide with the capillaries was placed on the automated motorized stage of a fluorescent laser microscope and covered with a hotplate heated to 37 °C. Images were taken every 15 min following excitation with a 445 nm laser.

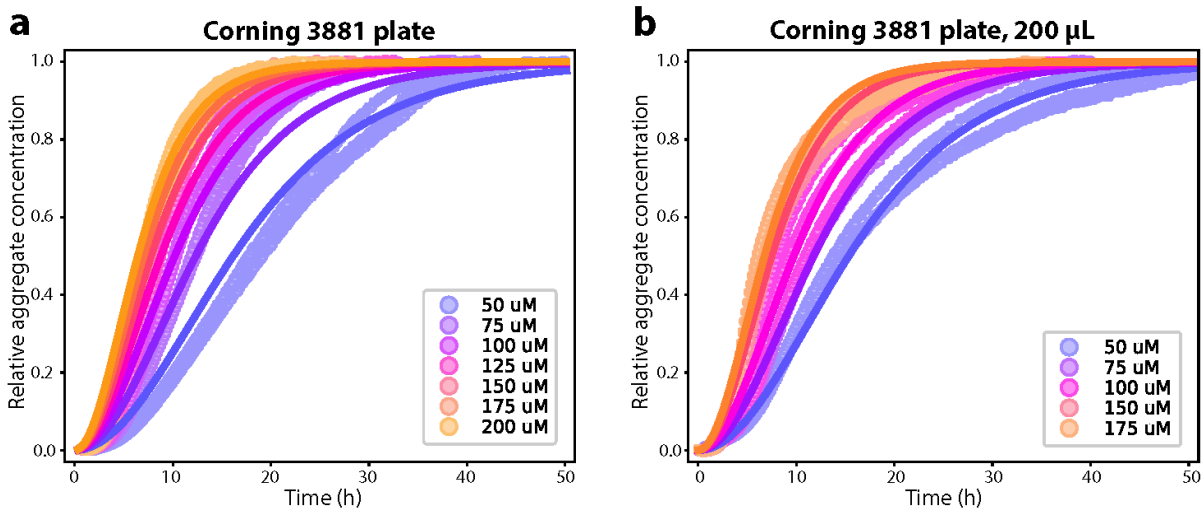

Supplementary Figure 2: Aggregation kinetics of FapC as measured by ThT is highly reproducible. A: Aggregation of FapC, same data as main text Fig. 4A. The kinetic data is well-fitted (MRE = 0.00287) by a nucleation-elongation model with n_c = 1.31, $k_n k_+$ = 1340 $M^{-1}h^{-2}$. **B**: Aggregation of FapC, separate experiment performed on a separate day but using the same reaction conditions apart from an increase fill height in the plate wells. Data look almost identical and is well-fitted (MRE = 0.00107) by a nucleation-elongation model with almost identical rate parameters n_c = 1.31, $k_n k_+$ = 1460 $M^{-1}h^{-2}$. This is the strongest of many examples throughout the study of the high reproducibility of the kinetics of FapC aggregation as measured by ThT fluorescence, when following the protocols outlined in Methods.

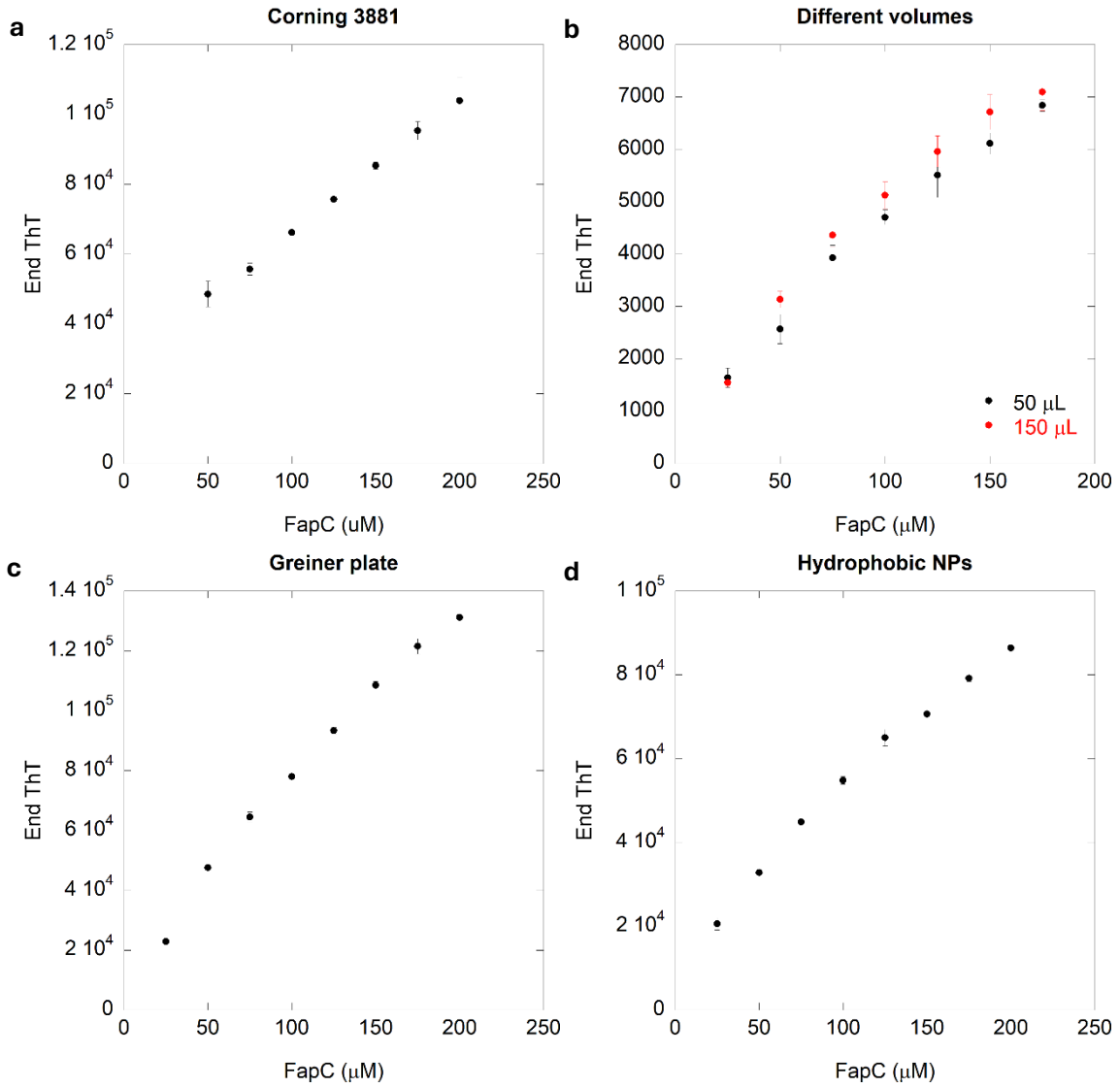

Supplementary Figure 3: Correlation between end-ThT level and initial FapC monomer concentration. A: Corning 3881 standard plate. **B**: Corning 3881 standard plate with different volumes of FapC. **C**: Greiner plate. **D**: FapC with a fixed concentration of hydrophobic nanoparticles. For all experiments a linear correlation is seen between the end-ThT level and the initial monomeric concentration of FapC indicating that ThT fluorescence intensity is correlated to the amount of aggregates formed in all experiments. As expected, the y-intercept is greater than zero in all cases. This originates from the baseline ThT fluorescence signal in the absence of fibrils (and of monomeric protein) that is always present. This baseline does not affect the analysis because during data processing we first subtract the baseline and then normalize the resultant baseline-subtracted data.[1]

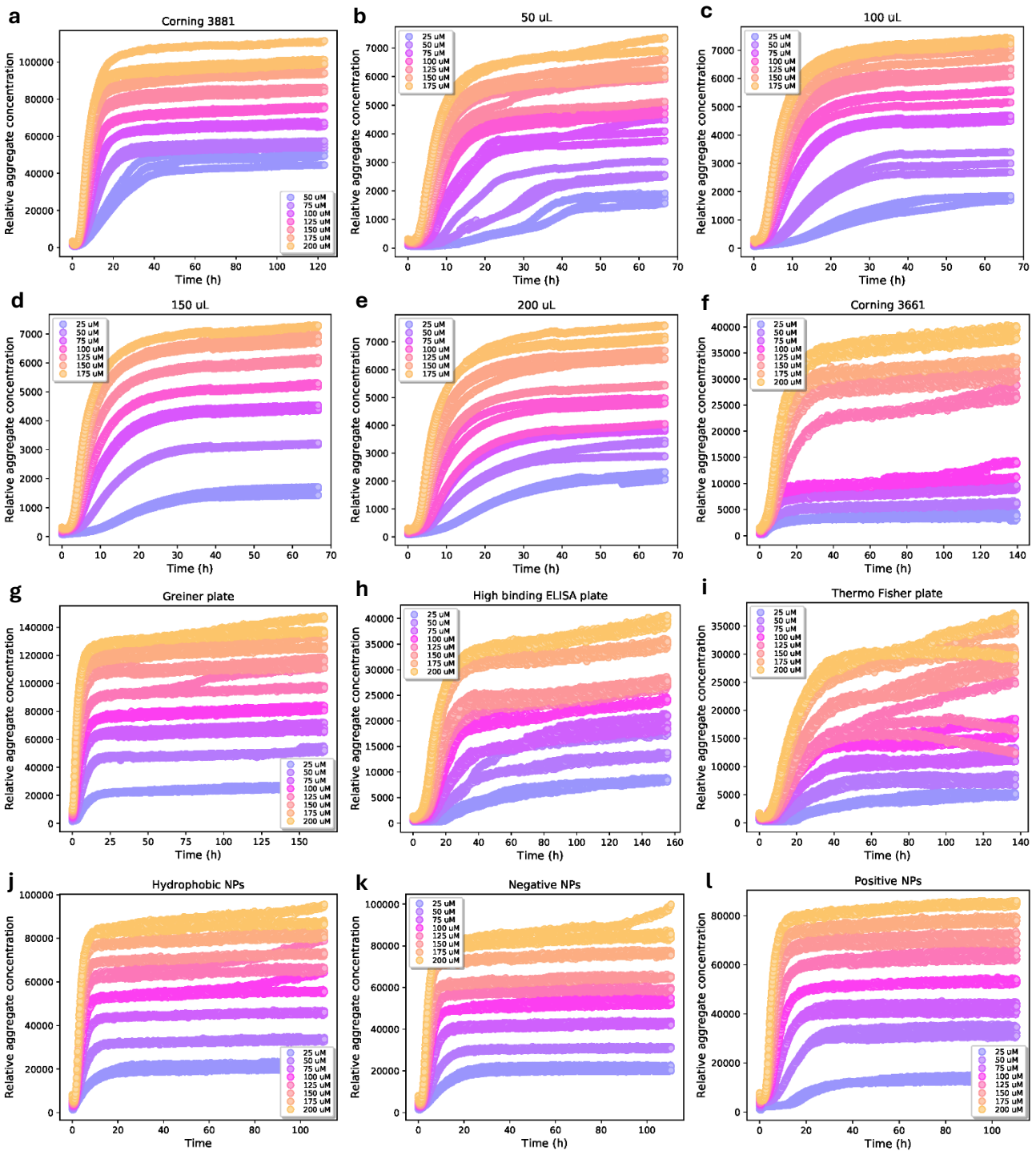

Supplementary Figure 4: Un-normalized full data set for all FapC plate reader experiments. A: Standard Corning 3881 plate. **B**: 50 µL FapC in the standard Corning 3881 plate. **C**: 100 µL FapC in the standard Corning 3881 plate. **D**: 150 µL FapC in the standard Corning 3881 plate. **E**. 200 µL FapC in the standard Corning 3881 plate. **F**: Corning 3661 plate. **G**: Greiner plate. **H**: High binding ELISA plate. **I**: Thermo Fisher plate. **J**: FapC with a fixed concentration of hydrophobic NPs. **K**: FapC with a fixed concentration of negative NPs. **L**: FapC with a fixed concentration of positive NPs. Note, the plateau in the ThT fluorescence at the end of the reaction contains no information about the reaction kinetics, although it can be affected by irrelevant external factors such as evaporation. Also, when the plateau phase is much longer than the important sigmoid phase, the latter is visually obscured in the plots. Therefore, it is generally desirable to truncate the data to remove much of the plateau. In Fig. S5 we have

done so for a standardized 50 h, which is late enough for almost all aggregation reactions measured to have completed, whilst being early enough to remove the majority of the plateau and to remove most artefacts introduced by evaporation.

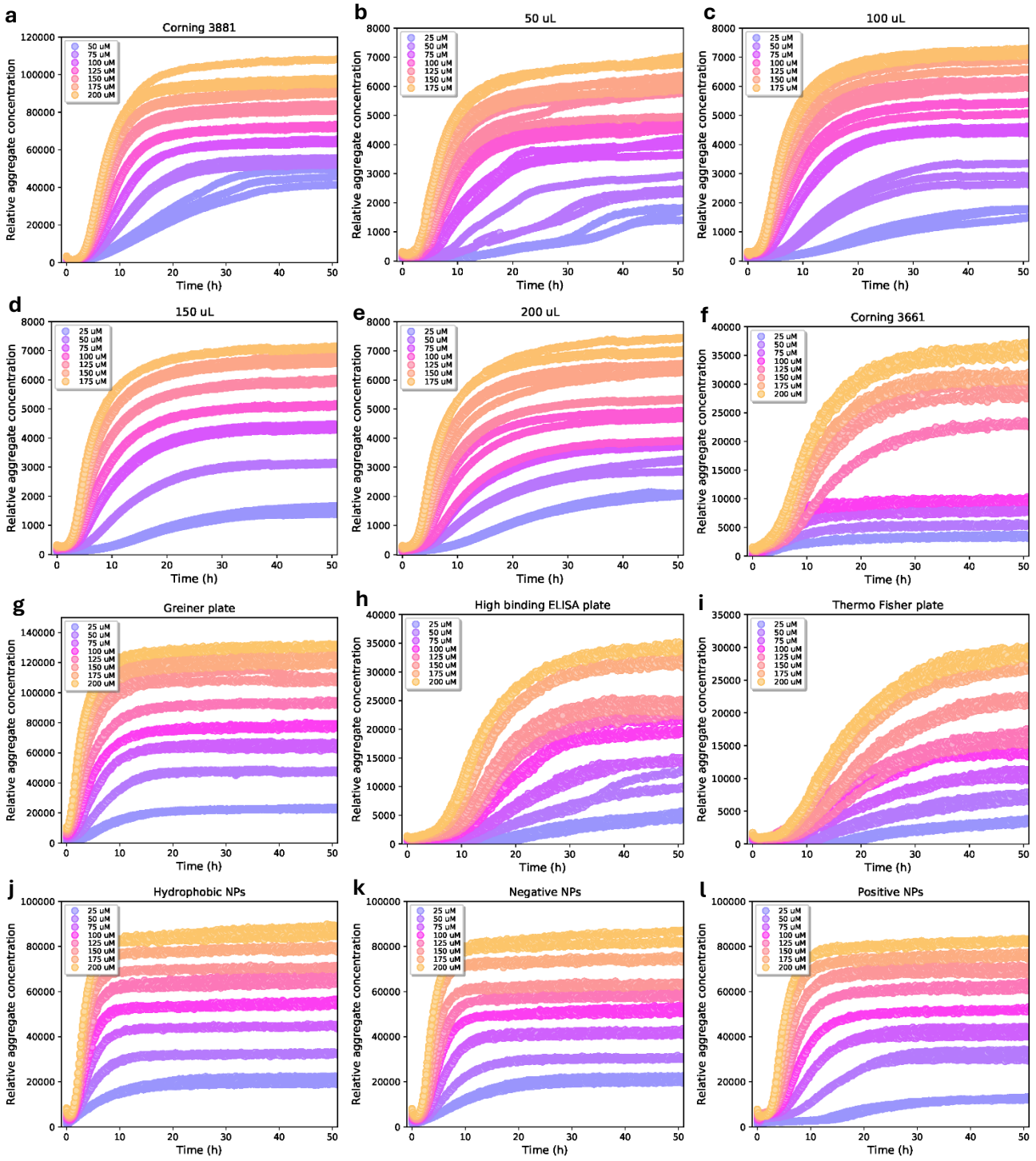

Supplementary Figure 5: Un-normalized full data set for all FapC plate reader experiments truncated after 50 h. A: Standard Corning 3881 plate. **B**: 50 µL FapC in the standard Corning 3881 plate. **C**: 100 µL FapC in the standard Corning 3881 plate. **D**: 150 µL FapC in the standard Corning 3881 plate. **E**. 200 µL FapC in the standard Corning 3881 plate. **F**: Corning 3661 plate. **G**: Greiner plate. **H**: High binding ELISA plate. **I**: Thermo Fisher plate. **J**: FapC with a fixed concentration of hydrophobic NPs. **K**: FapC with a fixed concentration of negative NPs. **L**: FapC with a fixed concentration of positive NPs.

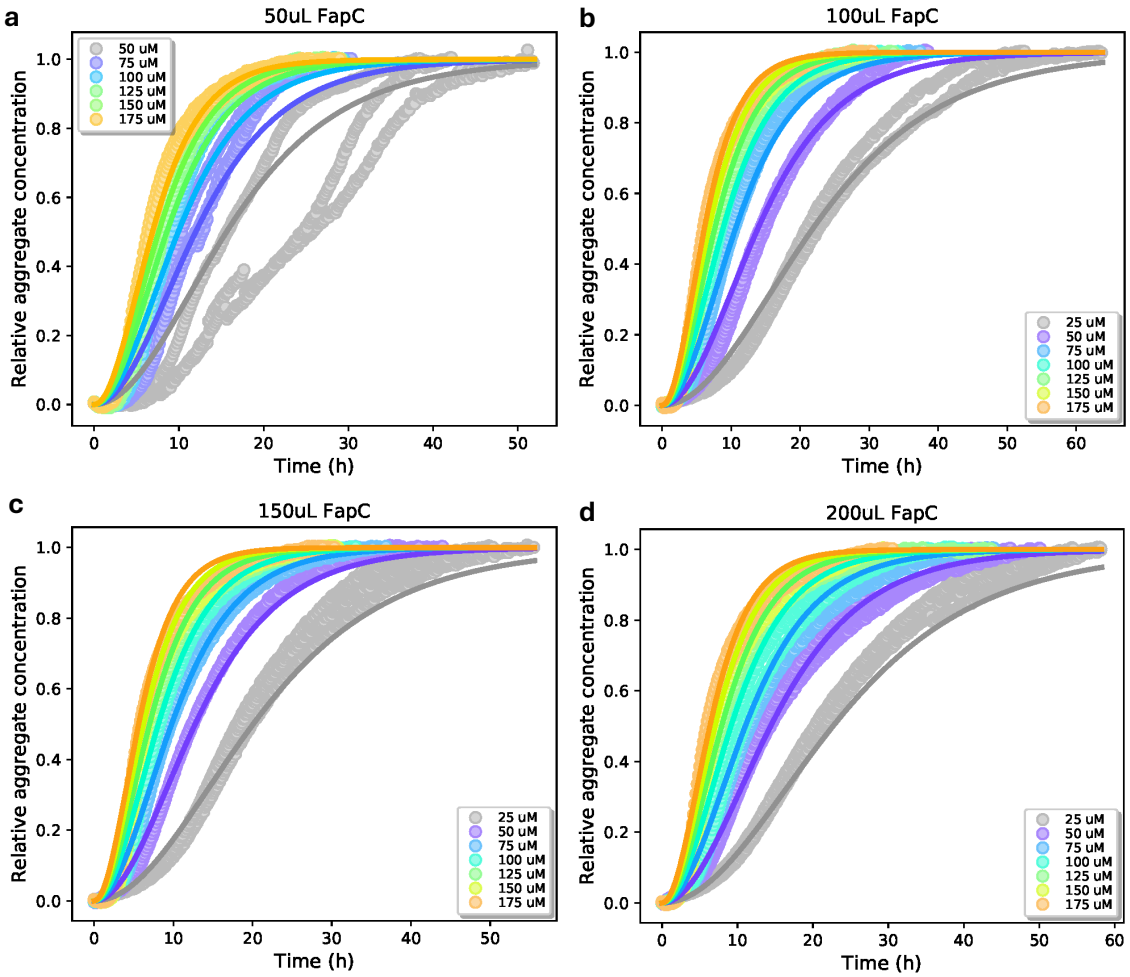

Supplementary Figure 6: Aggregation of FapC with different volumes in the wells of a 96-well microtiter plate. **A**: Aggregation of FapC with 50 µL of each sample loaded in each well. The data is fitted to a nucleation-elongation kinetic model with n_c as a global constant and k_nk_+ as a global fit. n_c = 1.31, k_nk_+=1.42 x 10^3 $M^{-1}h^{-2}$, MRE=0.00789. **B**: Aggregation of FapC with 100 µL of each sample loaded in each well. The data is fitted to a nucleation-elongation kinetic model with n_c as a global constant and k_nk_+ as a global fit. n_c = 1.3, k_nk_+=1.81 x 10^3 $M^{-1}h^{-2}$, MRE=0.00104. **C**: Aggregation of FapC with 150 µL of each sample loaded in each well. The data is fitted to a nucleation-elongation kinetic model with n_c as a global constant and k_nk_+ as a global fit. n_c = 1.31, k_nk_+=2.13 x 10^3 $M^{-1}h^{-2}$, MRE=0.00163. **D**: Aggregation of FapC with 200 µL of each sample loaded in each well. The data is fitted to a nucleation-elongation kinetic model with n_c as a global constant and k_nk_+ as a global fit. n_c = 1.31, k_nk_+=1.67 x 10^3 $M^{-1}h^{-2}$, MRE=0.00154.

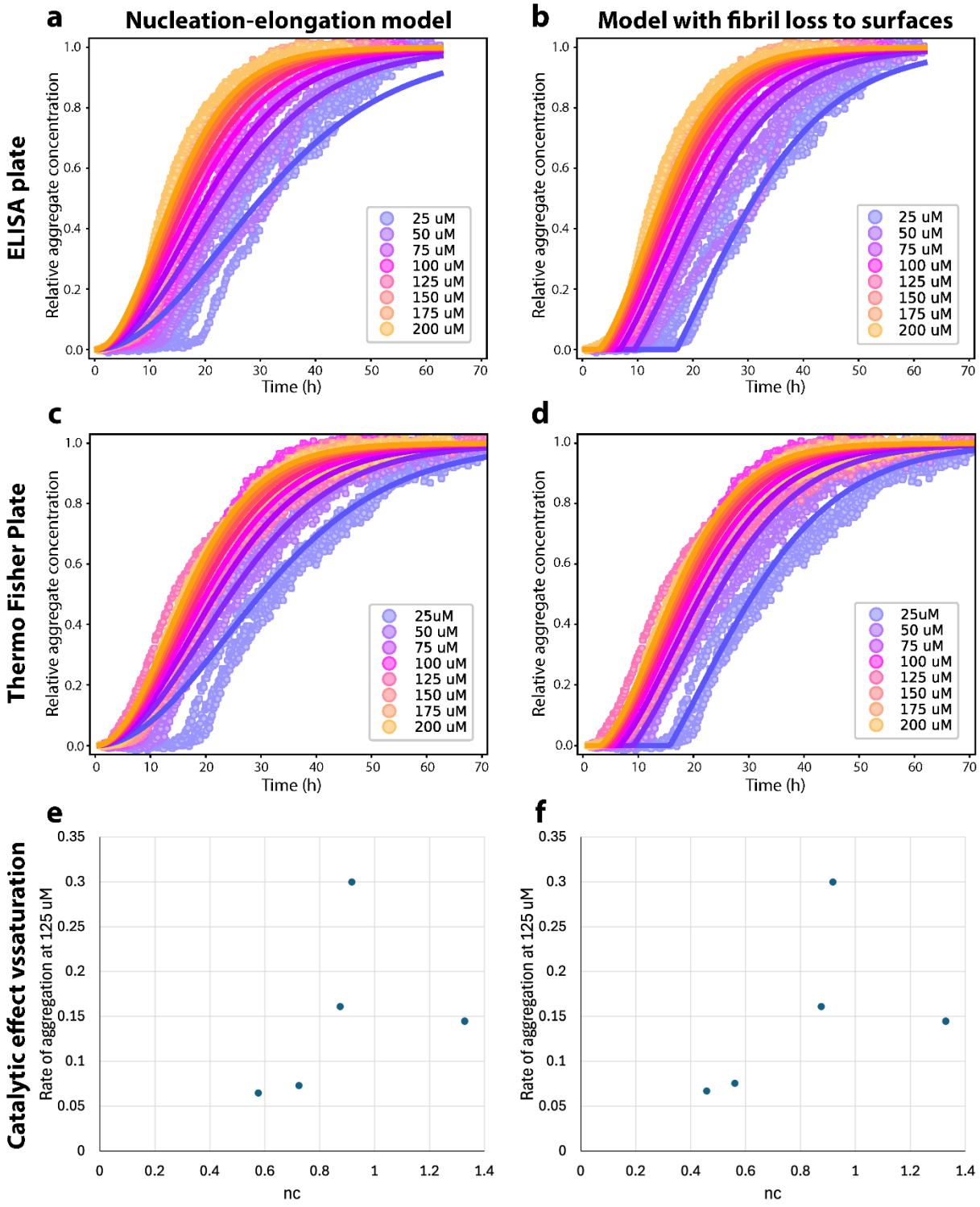

Supplementary Figure 7: Alternative kinetic model for aggregation in ELISA and Thermo Fisher plates. A: Aggregation of FapC in ELISA plate, same data as Fig. 4D but with 25 and 50 μM datasets included. The kinetic data are fairly well-fitted (MRE = 0.00470) by a nucleation-elongation model with n_c = 0.73, $k_n k_+$ = 1.8 $M^{-1}h^{-2}$, although the lowest two concentrations are much less well-fit. **B**: Same data as (A), but fitted to a provisional new kinetic model in which the first S μM of fibril mass formed adheres to the plate surface and is either not illuminated by the plate light source, or is not capable of binding ThT (Eqs. (S2)-(S3)). This yields better fits (MRE = 0.00304), particularly for the lowest concentrations, with rate parameters n_c = 0.56, $k_n k_+$ = 0.43 $M^{-1}h^{-2}$, S = 7.0 μM. **C**: Aggregation of FapC in Thermo Fisher plate,

same data as Fig. 4D but with 25 and 50 μM datasets included. The kinetic data are fairly well-fitted (MRE = 0.00333) by a nucleation-elongation model with n_c = 0.58, k_nk_+ = 0.37 $M^{-1}h^{-2}$, although the lowest two concentrations are much less well-fit. **D**: Same data as (C), but fitted to a provisional new kinetic model in which the first *S* μM of fibril mass formed adheres to the plate surface (Eqs. (S2)-(S3)). This yields better fits (MRE = 0.00234), particularly for the lowest concentrations, with rate parameters n_c = 0.46, k_nk_+ = 0.14 $M^{-1}h^{-2}$, *S* = 5.8 μM. **E-F**: The change in model has little qualitative effect on the relationship between primary nucleation rate and catalytic binding site affinity (degree of saturation of catalytic site). Although the fit to the new kinetic model is better, the improvement in fit is insufficient to positively confirm that fibrils stick to the surfaces of these plates. However, it does increase the likelihood that this is occurring.

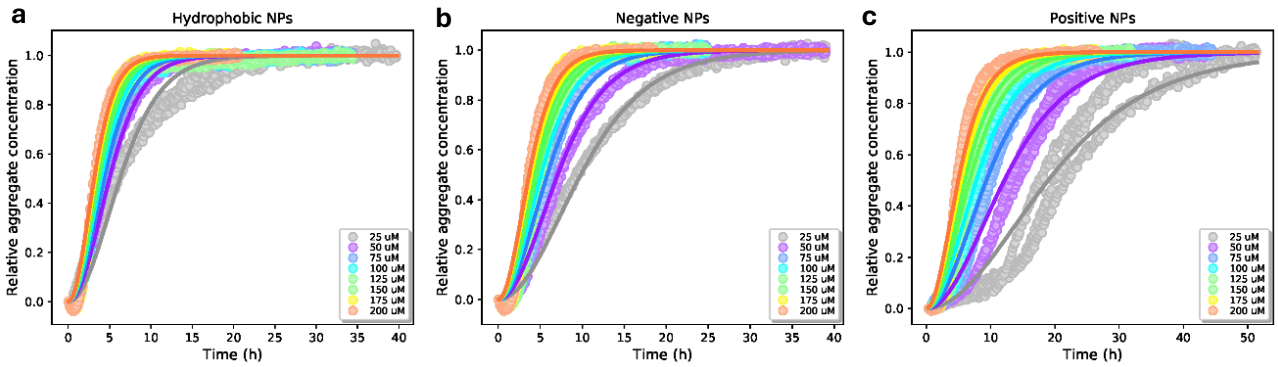

Supplementary Figure 8: Aggregation kinetics of FapC in the presence of NPs. A: Aggregation of FapC ranging from 25 μM to 200 μM FapC in the presence of a constant amount of hydrophobic NPs corresponding to a 1000:1 surface ratio of FapC to NP at 50 μM FapC. The kinetic data is nicely fitted to a nucleation-elongation model with n_c = 0.669, k_nk_+ = 23.0 $M^{-1}h^{-2}$, MRE = 0.00112. **B**: Aggregation of FapC ranging from 25 μM to 200 μM FapC in the presence a constant amount of negative NPs corresponding to a 5000:1 surface ratio of FapC to NP at 50 μM FapC. The kinetic data is nicely fitted to a nucleation-elongation model with n_c = 0.948, k_nk_+ = 185 $M^{-1}h^{-2}$, MRE = 0.00178. **C**: Aggregation of FapC ranging from 25 μM to 200 μM FapC in the presence of a constant amount of positive NPs corresponding to a 1000:1 surface ratio of FapC to NP at 50 μM FapC. The kinetic data is nicely fitted to a nucleation-elongation model with n_c = 1.29, k_nk_+ = 1.89 x 10^3 $M^{-1}h^{-2}$, MRE = 0.00341 corresponding to the kinetic parameters for fitting FapC in the absence of NPs.

Supplementary Table 1: Kinetic parameters for fitting 50 μM FapC in the presence of charged NPs to a nucleation-elongation model with n_c = 1.31 as a global constant and k_nk_+ fitted to each individual NP surface ratio.

Hydrophobic NP (MRE=0.00067)		Negative NP (MRE = 0.00306)		Positive NP (MRE = 0.00123)	
NP surface ratio	k_nk_+ ($M^{-1}h^{-2}$)	NP surface ratio	k_nk_+ ($M^{-1}h^{-2}$)	NP surface ratio	k_nk_+ ($M^{-1}h^{-2}$)
0:1	5.04 x 10^3	0:1	4.94 x 10^3	0:1	1.98 x 10^3
50:1	4.92 x 10^5	50:1	5.93 x 10^5	10:1	2.11 x 10^3
100:1	5.38 x 10^5	100:1	5.18 x 10^5	25:1	2.24 x 10^3
500:1	1.33 x 10^5	500:1	1.17 x 10^5	50:1	1.60 x 10^3
1000:1	6.90 x 10^4	1000:1	6.54 x 10^4	100:1	1.33 x 10^3
5000:1	1.14 x 10^4	5000:1	2.04 x 10^4	250:1	784
10000:1	1.03 x 10^4	10000:1	1.58 x 10^4	1000:1	1.20 x 10^3
50000:1	5.40 x 10^3	50000:1	6.72 x 10^3		
100000:1	6.41 x 10^3				

Alternative kinetic model

In Fig. S7 we fit the data from the Thermo Fisher and ELISA plates using a proposed model in which the plate walls strongly bind fibrils, where they do not fluoresce significantly. The maximum mass concentration of fibrils that can fit on the plate walls (i.e. the plate wall stoichiometry) is taken to be *S* μM. It is assumed that the binding is rapid on the timescale of aggregation kinetics such that it can be modelled as being at equilibrium. It is also assumed that the tight-binding limit holds, and thus that at any given time the maximum possible fibril concentration is bound. Finally, it is assumed that this binding does not greatly affect elongation. Under these conditions the rate laws are given by:

$$\frac{dP}{dt} = k_n m(t)^{n_c}, \quad \frac{dM}{dt} = 2k_+ m(t)P(t), \quad M(t) + m(t) = m_{tot}, \tag{S1}$$

$$M_f(t) = \begin{cases} 0, & M(t) < S \\ M(t) - S, & M(t) \geq S \end{cases} \tag{S2}$$

In these equations, notation follows previous works in the field. So, *P*, *M* and *m* are the number and mass concentrations of fibrils and the monomer concentration respectively; k_n and k_+ are the rate constants for primary nucleation and elongation, and n_c the reaction order of primary nucleation. M_f is the detectable fibril mass concentration. Since Eqs. (S1) are unmodified from their form in the standard nucleation-elongation model, the analytical solution for Eqs. (S1)-(S2) in the absence of preformed fibrils at t=0 is simply Eq. (S2) combined with the Oosawa solution [cite Meisl 2016 Nature Protocols]:

$$M(t) = m_{tot}\left(1 - \cosh\left(\sqrt{\frac{n_c}{2}}\lambda t\right)^{-\frac{2}{n_c}}\right), \quad \lambda = \sqrt{2k_+ k_n {m_{tot}}^{n_c}}. \tag{S3}$$

1. G. Meisl, J. B. Kirkegaard, P. Arosio, T. C. Michaels, M. Vendruscolo, C. M. Dobson, S. Linse and T. P. Knowles, *Nature protocols*, 2016, **11**, 252-272.